Chapter 5

Vitamin D Affects Neuronal Peptides in Neurodegenerative Disease: Differences of V-D2 and V-D3 for Affinity to Amyloid-β and Scrapie Prion Protein In Vitro

Yoichi Matsunaga, Midori Suenaga,
Hironobu Takahashi and Akiko Furuta

Additional information is available at the end of the chapter

http://dx.doi.org/10.5772/64508

Abstract

The misfolding of neuronal peptides such as Aβ40/42 in Alzheimer's disease and cellular prion protein in scrapie induce abnormal aggregation of the peptides in the brain. The seeding of peptides' oligomers from monomers is the initial step to form molten-globule states before abnormal aggregation. Therefore, compounds targeting the step are useful to clarify the mechanisms underlying aggregation of the proteins and Vitamin D derivatives, which can interact with both Aβ40 and cellular prion protein; however they show different effects in the oligomerization step of the proteins. We discuss the different effects of Vitamin D_2 and Vitamin D_3 in the interaction with these peptides in brain.

Keywords: Alzheimer's disease, prion disease, amyloid-β, human PrP^c, Vitamin D derivatives, oligomerization

1. Introduction

Recently, involvement of Vitamin D (V-D) in cognitive impairment is reported.

V-D is a secosteroid and occurs in two distinctive major forms: Vitamin D_2 (V-D_2) and Vitamin D_3 (V-D_3). V-D_3 is a 27-carbon derivative of cholesterol, and V-D_2 is a 28-carbon derivative from plant ergosterol. The structure of V-D_2 differs from V-D_3 by containing an extra methyl group and a double bond between carbon 22 and 23 (**Figure 1**). Both V-D derivatives appear to have

similar biological effects in humans [1, 2]. V-D_3 is about four times as potent as V-D_2 [3]. Interestingly, V-D_2 is a naturally occurring V-D form derived from a fat extract of yeast by the exposure to UV light, and the metabolites were not detectable in the blood of vertebrates such as humans, unless administered from an external source [3, 4]. Thus, V-D_2 is not synthesized in vivo and is regarded as a supplement. The metabolites derived from V-D_2 are not equivalent to those for V-D_3 [5]. In contrast to V-D_2, V-D_3 is the naturally synthesized within the skin and oils of fur. Although both microsomal and mitochondrial 25-hydroxylases act on V-D_3, they do not act on V-D_2 [4, 6, 7], and furthermore the V-D binding protein shows lower affinity for V-D_2 than V-D_3 and its metabolites [8]. Currently, clinical applications of V-D for immunosuppression and reduction of pro-inflammatory immune pathways demonstrate that V-D is a prosteroid hormone rather than a vitamin [9, 10]. V-D cross blood-brain barrier by passive diffusion and enter the cerebrospinal fluid and brain. The beneficial effects in reducing the relapse risk in multiple sclerosis through its immune-regulatory effects were reported [11].

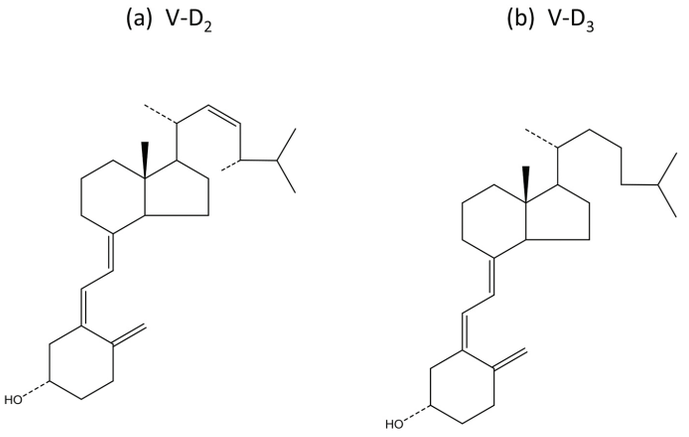

Figure 1. Structural differences between Vitamin D_2 and Vitamin D_3.

Recent epidemiologic studies report V-D_3 deficiency as a risk factor of cardiovascular disease including cardiac hypertrophy, myocardial remodeling developed to heart failure (HF) [12, 13] and some prospective studies report the relationship between hypovitaminosis-D and an increased risk of cognitive decline in elderly population [14] and suggested that supplementation of V-D could prevent the cognitive disorders [15–17], and its effects for the clearance of aggregated amyloid-β (Aβ) in AD brain [18].

In this chapter, we present the different binding affinity of V-D_2 and V-D_3 to amyloidogenic protein in brain: Aβ and prion protein.

2. Amyloid-β protein in Alzheimer's disease and scrapie prion protein in prion disease

AD and prion diseases are neurodegenerative diseases in brain and cause dementia. AD is the most common case of senile dementia and the number of AD patients is increasing and recent

http://dx.doi.org/10.5772/64508

study shows that 46.8 million of AD patients live in the world and it is estimated to reach 131.5 million by 2050 [19]. It is featured by memory loss, deterioration of cognitive and behavioral process, and diminished social life. These symptoms do not improve and progress with life time.

The main pathological hallmark with AD patients is the senile plaque in the brain [20]. Extracellular accumulation of insoluble Aβ protein is the main component of the plaque that induces synaptic dysfunction and neuronal loss resulting in progressive dementia [21]. The Aβ is composed of 39–43 amino acids, naturally produced by proteolytic cleavage of integral membrane protein, 100–135 kDa amyloid precursor protein [22]. The majority of the secreted Aβ alloform includes the C-terminal Aβ40 and Aβ42. Quantitative analyses have shown that, on average, 60% of all plaques contain Aβ42 and 31% contain Aβ40 [23]. The misfolding and aggregation of Aβ and tau proteins are two principal aggregating proteins in AD brain [24, 25]. Growth of the fibrils occurs by assembly of the Aβ seeds into intermediate protofibrils, and self-associates to form mature fibers [26]. This multistep process may be influenced at various stages by factors that promote Aβ fiber formation and aggregation, and the seeding of Aβ40 oligomers is the initial step of the process [27, 28].

The emergence of a prion disease in cattle is known as bovine spongiform encephalopathy (BSE) and a possible transmission to humans by the exposure to BSE has been suggested [29, 30]. Gerstmann-Straussler-Scheinker disease and Creutzfeldt-Jacob are well-known naturally occurring prion diseases in human and they are transmissible and fatal. The main event contributing to the pathogenesis of prion disease is the conversion of the cellular prion protein (PrP^{c}) into scrapie prion protein (PrP^{sc}), which is a protease-resistant, insoluble protein [31, 32]. PrP^{c} is predominantly expressed in neurons, and attached to extracellular space of plasma membrane through a glycophosphatidylinositol. It is a sialoglycoprotein with a molecular weight of approximately 33–35 kDa [33, 34]. Studies have shown that PrP^{c}(90–231), which is N-terminal truncated fragments of PrP^{c} and corresponds to the core of the protease K (PK) resistant prion protein, preserve the pathogenic features of PrP^{sc} [35, 36]. Gerstmann-Straussler-Scheinker disease and Creutzfeldt-Jacob disease are caused by mutations in the PrP gene [37] and the mutations directly link to conformational conversion from PrP^{c} to PrP^{sc} and amplification of PrP^{sc} without exogenous PrP^{sc} [38, 39], and the infectivity can be explained by the direct PrP^{sc}-PrP^{c} interaction [40]. In vitro generation of infectious PrP^{sc} has demonstrated the protein-only hypothesis of prion propagation [41, 42]. Many reports have suggested that the multistep process of conversion from PrP^{c} into PrP^{sc} includes an oligomerization/polymerization step [43, 44]. The oligomerization or molten-globule state is a preliminary step required for the formation of insoluble protein in the brain like that of Aβ aggregates in AD brain, and soluble oligomers appear to be more cytotoxic than mature aggregates [45].

2.1. V-D-induced Aβ40 oligomerization

Quartz-crystal microbalance (QCM) measurement is a highly sensitive mass-measuring system [46, 47]. The instrument is equipped with a 27 MHz QCM plate at the bottom with a stirring bar. Changes of frequency are calculated by Sauerbrey's equation [48] as below.

We applied Sauerbrey's equation for the QCM in the air phase:

$$\Delta F = -2F_0^2 \Delta m / A\sqrt{\rho_q \cdot \mu_q}$$

where ΔF is measured frequency change (Hz), Δm is mass change, F_0 is fundamental frequency of the quartz-crystal, A is an electrode area, ρ_q is density of quartz-crystal, and μ_q is the shear modulus of quartz-crystal.

The equation indicates that a 0.61 ng/cm^2 increase in mass means a −1 Hz decrease in frequency. The change of frequency is proportional to that of mass.

The change of mass in Aβ40 with V-D_2 or V-D_3 was determined [49]. A significant decrease in frequency started after 15 min upon addition of Aβ40 to the V-D_2 solution, and found that the frequency decrease depends on both V-D_2 concentration and incubation time. Aβ40-V-D_2 complex formation occurs in solution and accelerated after 15–60 min later (**Figure 2a**). After 60 min, the calculated Aβ40 molecules aggregated by an Aβ40 was 4.21394 e^{19} at 0.1 M of V-D_2, 6.74725 e^{19} at 0.5 μM of V-D_2, and 8.85697 e^{19} at 1.0 μM of V-D_2 (**Table 1**). In case of V-D_3, however, no considerable decrease in frequency upon Aβ40 addition was observed (**Figure 2b**). These results show a different potential of V-D_2 and V-D_3 for Aβ40 oligomerization in vitro.

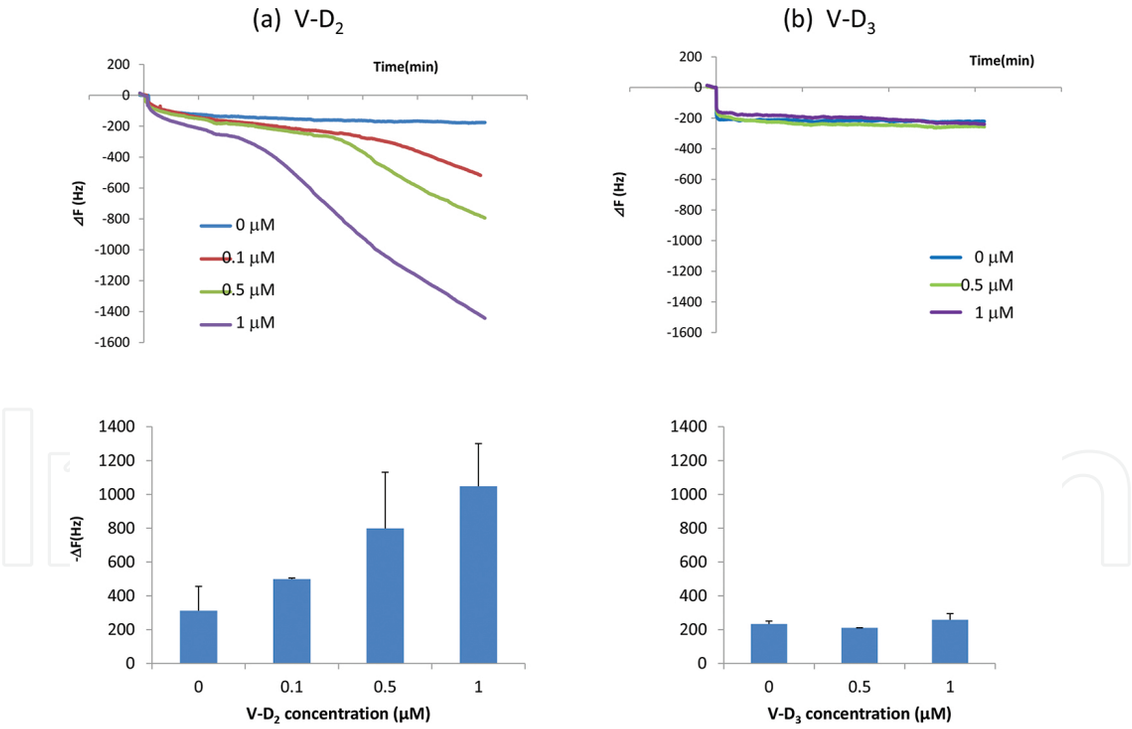

Figure 2. Quartz-crystal microbalance pattern for Aβ40 aggregation with V-D derivatives. Typical real-time monitoring of Aβ40 (12 μM) aggregation with V-D_2 at the concentrations of 0, 0.1, 0.5, and 1 μM (a) or with V-D_3 at the concentrations of 0, 0.5, and 1 μM (b) in quartz-crystal microbalance measurements. The changes of frequency of Aβ40 with V-D_2 or V-D_3 for 60 min are shown. The data are representative of three experiments. Total amount of Aβ40 aggregates with V-D_2 (a). V-D_2 induced potential dose-dependent Aβ40 aggregates. Total amount of Aβ40 aggregates with V-D_3 (b). V-D_3 did not induce Aβ40 aggregation after 60 min.

V-D_2 (μM)	−Δ*F* (Hz)	Δ*m* (ng/cm²)[a]	Δ*n* (atoms/cm²)[b]
Control*	3111 ± 44	190	2.63507×10^{19}
0.1	498 ± 6	304	4.21394×10^{19}
0.5	798 ± 332	487	6.74725×10^{19}
1	1048 ± 252	639	8.85697×10^{19}

* Direct binding of Aβ40 peptide to the Au electrode without V-D_2.
[a] A 1 Hz decrease in frequency results in a 0.61 ng/cm² increase in mass.
[b] Calculation using a molecular weight of 4331 for Aβ40.
Data are presented as mean ± SD values for three independent experiments.

Table 1. Measurement of frequency decrease in Aβ40 aggregation by V-D_2 on performing QCM 60 min later.

2.2. Electron microscopic observation exhibited V-D_2-induced Aβ40 oligomerization

Aβ40 in artificial cerebrospinal fluid without V-D as a control induced weak self-oligomerization and V-D_3 induced no enhancement to the control, however V-D_2 enhanced potent oligomerization for Aβ40 as **Figure 3**(**a–c**) [49].

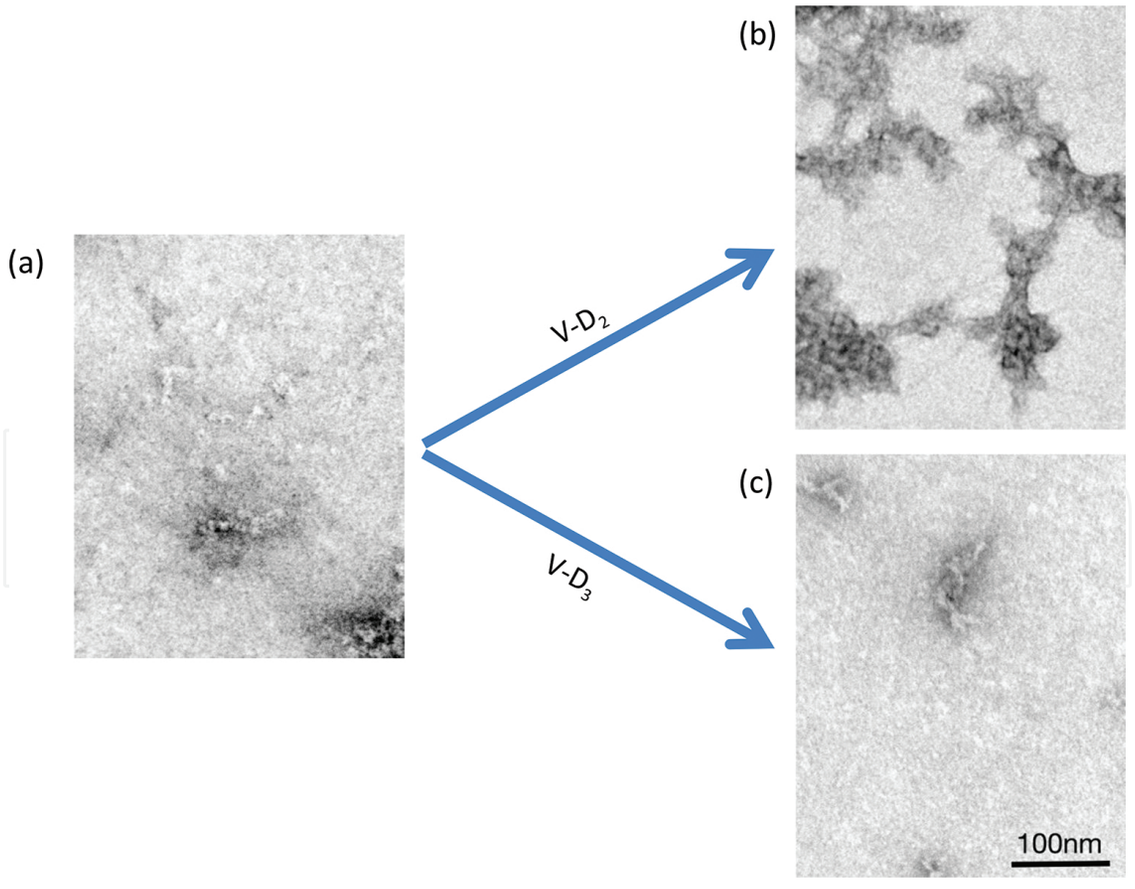

Figure 3. Electron microscopic observation for Aβ40 without or with V-D_2 or V-D_3. Aβ40 without V-D as a control (a), Aβ40 with V-D_2 (b), and Aβ40 with V-D_3 (c). Aβ40 in the photo indicates 100 nm for (a), (b), and (c).

2.3. Thioflavin-T assay revealed β-sheet formation of Aβ40 with V-D_2

Amyloid fibers are ordered β-sheet-rich proteins. Benzothiazole dye, Thioflavin-T (Th-T) is used to probe amyloid fibril formation due to specific noncovalent interactions that yield strong fluorescence upon binding [50]. Aβ40 showed a peak at 490 nm, indicating β-sheet formation [51]. V-D_2 increased peak intensity at 490 nm dose-dependently, indicating that V-D_2 facilitates β-sheet formation in Aβ40. The V-D_3 do not increase peak fluorescent intensity at 490 nm, indicating that V-D_3 facilitate no β-sheet formation in Aβ40 peptide (**Figure 4**) [49].

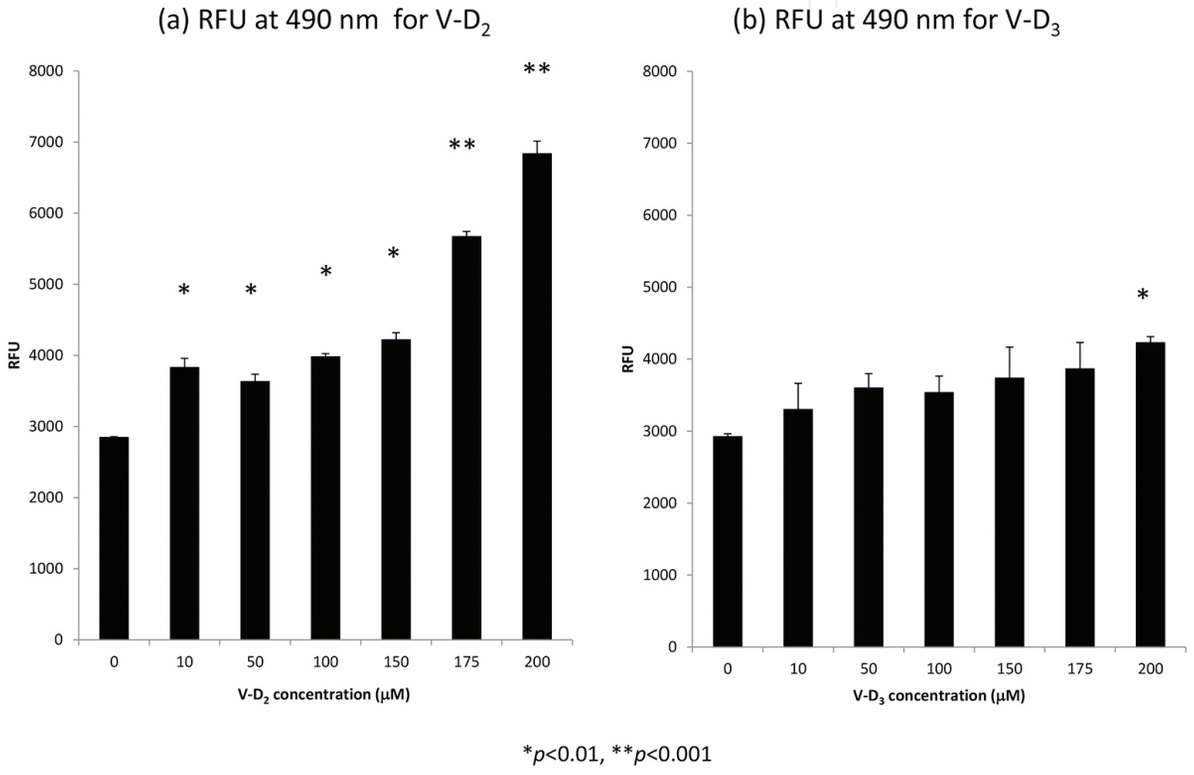

Figure 4. Th-T fluorescence monitored β-sheet formation of Aβ40 in the presence of V-D_2, V-D_3. (a) V-D_2 facilitates strong β-sheet formation in Aβ40 and (b) V-D_3 induced weak β-sheet formation in Aβ40. Y-axis indicates relative fluorescence units (RFUs). Data represent the mean ± SD values (bar) for three independent experiments. *p < 0.01, **p < 0.001 vs. without V-D derivatives.

2.4. Docking simulation between Aβ40 and V-D_2 or V-D_3

In silico docking analysis at the tertiary structure level by Molecular Operating Environment (MOE) software indicates the different interactions between V-D_2 or V-D_3 and Aβ40 peptide. The calculated minimum energy for V-D_2 was −40.36 kcal/mol and for V-D_3, −12.46 kcal/mol; for cholesterol, the calculated minimum energy was −25.89 kcal/mol. The result showed that both V-D_2 and V-D_3 bind common amino acid residues 7–8, 11–12, and 15–16 of Aβ40, and the C22–C23 double bond in V-D_2 stacks with the benzene ring of Phe19 in Aβ40, whereas V-D_3 has no double bonds and showed no stacking (**Figure 5**) [49].

http://dx.doi.org/10.5772/64508

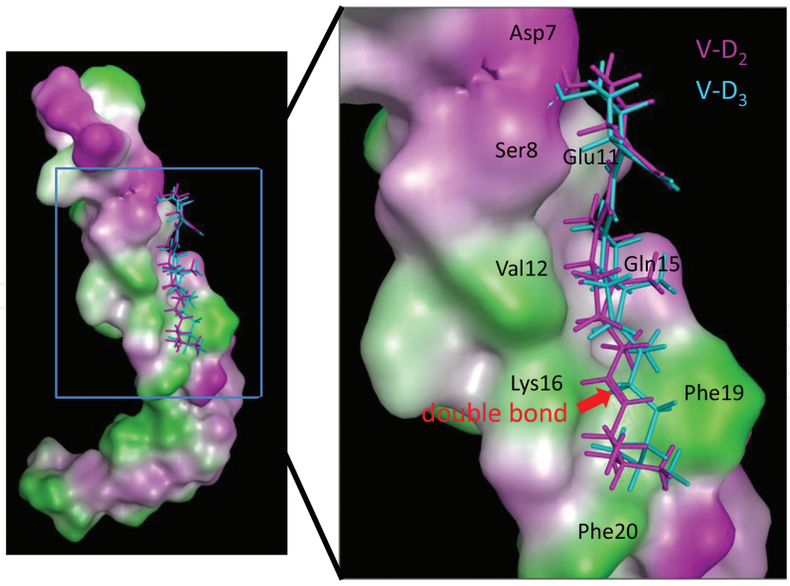

Figure 5. Docking simulation between Aβ40 and V-D_2 or V-D_3. Purple indicates hydrophilic residues and green indicates hydrophobic residues in Aβ40 (backbone). The double bonds (red arrow) of V-D_2 stack on the benzene ring of Phe19 in Aβ40. The minimum energy between Aβ40 and V-D_2 was −40.36 kcal/mol, that between Aβ40 and V-D_3 was −12.46 kcal/mol.

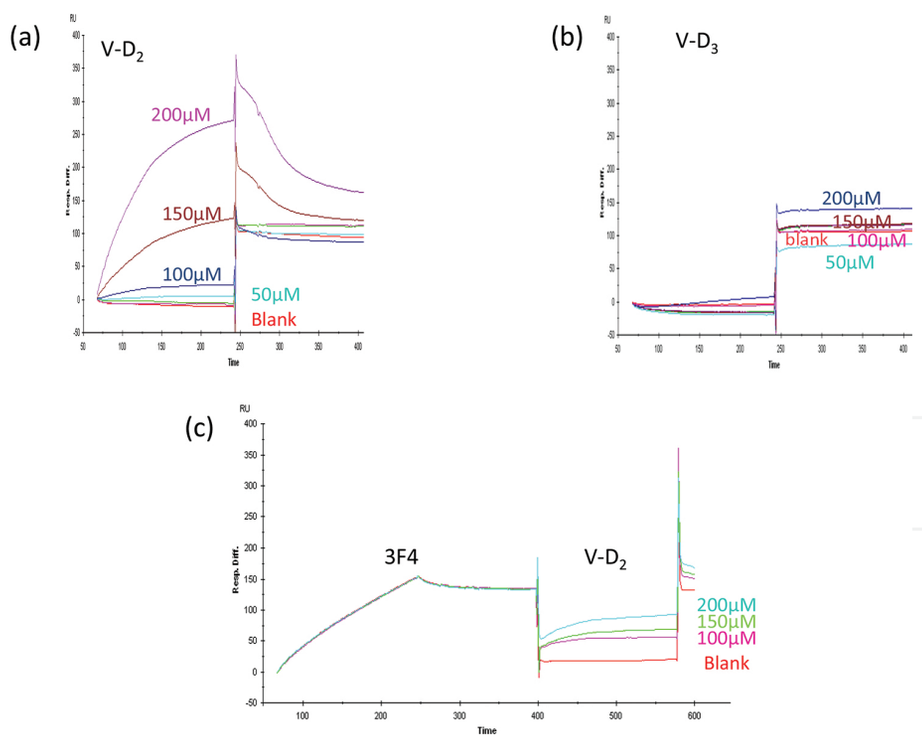

Figure 6. Affinity of V-D to PrP, as measured using the Biacore system. (a) The interaction between PrP^c(90–231) and V-D_2 showed high binding affinity, with a K_a of 6.17 e^8 and a K_d of 1.62 e^{-9}. (b) The interaction between PrP^c(90–231) and V-D_3 showed no binding affinity. (c) The interaction between PrP^c(90–231) and V-D_2, after saturating with the anti-3F4 mAb.

2.5. Affinity of V-D_2 to PrP^c(90–231), as a Biacore assay

A Biacore assay indicates a high affinity of V-D_2 for human recombinant cellular prion protein (Hu-rPrP^c)(90–231), and after saturating PrP^c(90–231) with the anti-3F4 antibody, specific for amino acid fragment 109–112 of PrP^c, V-D_2 binding to PrP^c(90–231) was decreased (**Figure 6a and c**), indicating that within the 3F4 epitope, PrP^c(90–231) was responsible for the interaction with V-D_2. However, V-D_3 showed no affinity for PrP^c(90–231) (**Figure 6b**), The binding kinetics of V-D_2 to Hu-rPrP^c(90–231) was shown in **Table 2** [52].

Ligand	Analyte	K_a (1/M)	K_d (M)
	V-D_2	6.17 e^8	1.62 e^{-9}
PrP^c(90–231)	V-D_3	ND*	ND*
	3F4 + V-D_2	1.12 e^8	8.95 e^{-9}

* ND, not detected.

Table 2. Binding kinetics of V-D_2 and V-D_3 to Hu-rPrP^c(90–231).

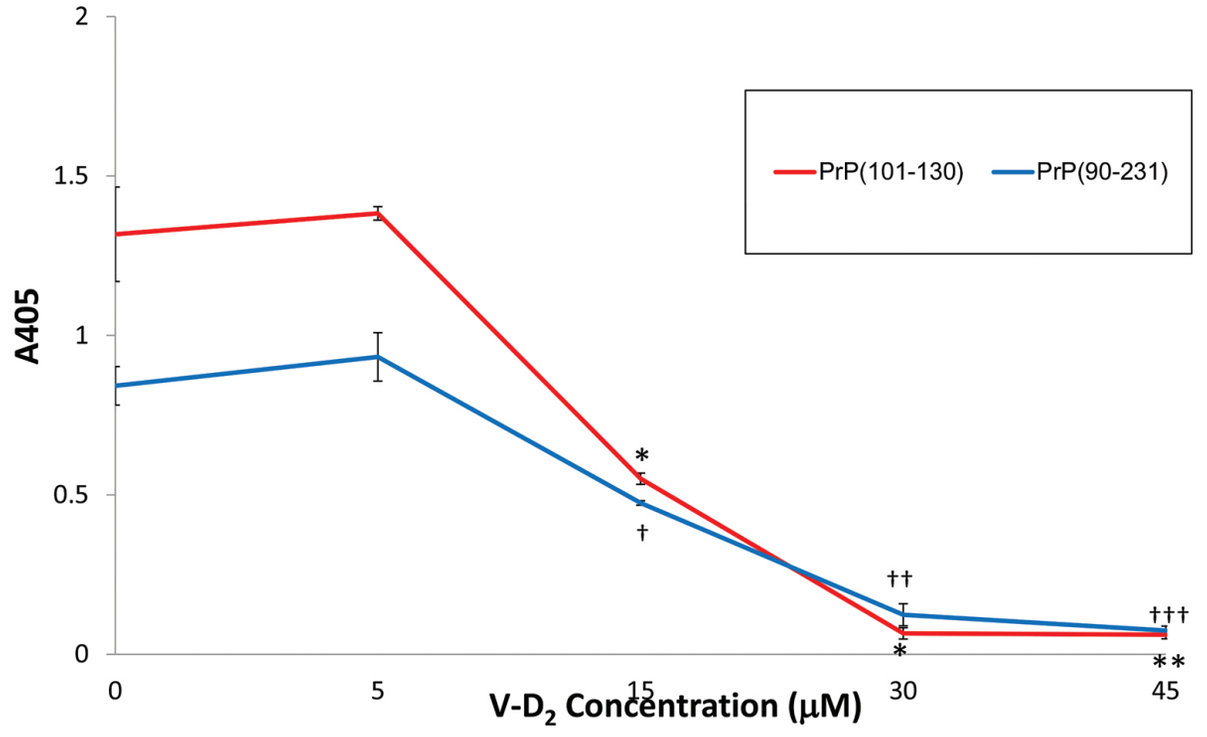

*p<0.006,**p<0.003 vs. PrP^c(101-130) without V-D_2,
†p<0.005, ††p<0.01, †††p<0.05 vs. Hu-rPrP^c(90-231) without V-D_2.

Figure 7. Reactivity of mAbs against PrP^c with V-D_2 by ELISA. The 3F4 epitope on PrP^c was affected by V-D_2 in a dose-dependent manner. The blue line indicates signals for PrP^c(90–231) and the red line f PrP^c(101–130).

2.6. Reactivity of 3F4 antibody with Hu-rPrP^c(90–231) bound to V-D_2, as monitored by ELISA

The responsible fragment within Hu-rPrP^c(90–231) that was affected by V-D_2 was determined by ELISA. The reactivity of the 3F4 antibody to PrP^c(90–231) that was incubated with V-D_2 showed decreasing signals toward PrP^c(90–231) bound with V-D_2 in a dose-dependent manner (**Figure 7**) [52]. These results confirm the observation by Biacore assay (**Figure 6**).

2.7. Specific sequences of Aβ40 and PrP^c(90–231) responsible to conformational transition

The Aβ hydrophobic core 16–20 (KLVFF) was the minimum sequence required in a binding screen of full-length and trimeric to decameric peptides spanning the entire Aβ40 sequence. Alanine substitution demonstrated that Lys16, Leu17, and Phe20 are critical for this interaction [53]. The stereospecific binding of KLVFF to the homologous Aβ sequence was later confirmed as the product of specific hydrophobic and electrostatic interactions. Controlling amyloid β-peptide fibril formation with protease-stable ligands was reported [53]. The sequences of Aβ (9–14): GYEVHH and Aβ (17–21): LVFFA, are responsible to pH-shifts [54] and thermal-induced structural transformation from α-helix/random coil to β-sheet in Aβs were Aβ (16–23) and Aβ (17–24) [55]. The conformational transition from Aβ40 monomer to oligomers may occur in response to small chemical compounds and may be dependent on specific Aβ40 sequences. The key amino acid of Aβ40 for interaction with V-D_2 is the Phe at a position 19, and it is around the sequences responsible to pH shifts and thermal stress [54, 55].

In case of PrP^c(90–231), the sequence of PrP^c(107–112): TNMKHM is pH dependent [56], and it contains PrP^c(109–112), the responsible sequence for the interaction with V-D_2.

2.8. Structural difference of V-D_2 and V-D_3 could explain different potential for the affinity to Aβ40 and PrP^c(90–231)

The C22–C23 double bond contained in V-D_2 structure may influence the conformational flexibility of the molecule through allylic strain and rigidity of the double bond against rotation [57, 58]. Therefore, we hypothesize that conformational restriction by the double bond in the V-D_2 side chain facilitated binding of V-D_2 to the recognition site of Aβ40 and PrP^c(90–231).

3. Conclusion

We detected V-D_2-induced Aβ40 oligomerization by QCM, and electron microscopic observation demonstrated the potential of V-D_2 for Aβ40 oligomerization through β-sheet formation as revealed by Th-T study. V-D_2-mediated Aβ40 oligomerization occurs through interaction between the Phe19 benzene ring of Aβ40 and the C22–C23 double bond of V-D_2. In case of prion, the fragment of V-D_2 binding to PrP^c(90–231) is around 3F4 epitope, 109–112 amino acid in PrP^c(90–231). These fragments are involved in the sensitive fragments to pH shifts and thermal stress. The binding of V-D_2 to amyloidogenic peptides in brain might give some insights to oligomerization of these peptides in the brain.

Author details

Yoichi Matsunaga[1*], Midori Suenaga[1], Hironobu Takahashi[1] and Akiko Furuta[2]

*Address all correspondence to: matsunaga@ph.bunri-u.ac.jp

1 Department of Medical Pharmacology, Faculty of Pharmaceutical Sciences, Tokushima Bunri University, Nishihama, Yamashiro-cho, Tokushima, Japan

2 Department of Psychiatry, Juntendo University, School of Medicine, Hongo, Bunkyo-ku, Tokyo, Japan

References

[1] Hunt, R. D.; Garcia, F. G.; Hegsted, D. M.; Kaplinsky, N. Vitamin D_2 and D_3 in new world primates: influence on calcium absorption. *Science* 157: 943–945; 1967.

[2] Steenbock, H.; Kletzien, S. W. F.; Haplin, J. G. The reaction of the chicken to irradiated ergosterol and irradiated yeast as contrasted with natural vitamin D of fish liver oils. *J Biol Chem* 97: 249–264; 1932.

[3] Trang, H. M.; Cole, D. E.; Rubin, L. A.; Pierratos, A.; Sui, S.; Vieth, R. Evidence that vitamin D_3 increases serum 25-hydroxyvitamin D more efficiently than does vitamin D_2. *Am J Clin Nutr* 68: 854–858; 1998.

[4] Marx, S. J.; Jones, G.; Weinstein, R. S.; Chrousos, G. P.; Renquist, D. M. Differences in mineral metabolism among nonhuman primates receiving diets with only vitamin D_3 or only vitamin D_2. *J Clin Endocrinol Metab* 69: 1282–1290; 1989.

[5] Mawer, E. B.; Jones, G.; Davies, M.; Still, P. E.; Byford, V.; Schroeder, N. J.; Makin, H. L. J.; Bishop, C. W.; Knutson, J. C. Unique 24-hydroxylated metabolites represent a significant pathway of metabolism of vitamin D_2 in humans: 24-hydroxyvitamin D_2 detectable in human serum. *J Clin Endocrinol Metab* 83: 2156–2166; 1998.

[6] Holmberg, I.; Berlin, T.; Ewerth, S.; Bjorkhem, I. 25-Hydroxylase activity in subcellular fractions from human liver. Evidence for different rates of mitochondrial hydroxylation of vitamin D_2 and D_3. *Scand J Clin Lab Invest* 46: 785–790; 1986.

[7] Guo, Y. D.; Strugnell, S.; Back, D. W.; Jones, G. Transfected human liver cytochrome P-450 hydroxylates vitamin D analogs at different side-chain positions. *Proc Natl Acad Sci USA* 90: 8668–8672; 1993.

[8] Jones, G.; Byrnes, B.; Palma, F.; Segev, D. Mazur, Y. Displacement potency of vitamin D_2 analogs in competitive protein-binding assays for 25-hydroxyvitamin D_3, 24,25-

dihydroxyvitamin D_3, and 1,25-dihydroxyvitamin D_3. *J Clin Endocrinol Metab* 50: 773–775; 1980.

[9] Tsoukas, C. D.; Provvedini, D. M.; Manolagas, S. C. 1,25-dihydroxyvitamin D_3: a novel immunoregulatory hormone. *Science* 224: 1438–1440; 1984.

[10] Lemire, J. M. Immunomodulatory actions of 1,25-dihydroxyvitamin D_3. *J Steroid Biochem Mol Biol* 53: 599–602; 1995.

[11] Simpson, S.; Taylor, B.; Blizzard, L.; Ponsonby, A. L.; Pittas, F.; Tremlett, H.; Dwyer, T.; Gies, P.; van der Mei, I. High 25-hydroxyvitamin D is associated with lower relapse risk in multiple sclerosis. *Ann Neurol* 68: 193–203; 2010.

[12] Kim, D. H.; Sabour, S.; Sagar, U. N.; Adams, S.; Whellan, D. J. Prevalence of hypovitaminosis D in cardiovascular disease; from the National Health and Nutrition Examination survey 2001 to 2004. *Am J Cardiol* 102: 1540–1544; 2010.

[13] Scragg, R. K.; Camargo, C. A.; Jr, Simpson, R. U. Relation of serum 25-hypovitamin D deficiency and risk of cardiovascular disease. *Am J Cardiol* 105: 122-128; 2010.

[14] Soni, M.; Kos, K.; Lang, I. A.; Jones, K.; Melzer, D.; Liewllyn, D. J. Vitamin D and cognitive function. *Scand J Lab Invest Suppl* 243: 79–82; 2012.

[15] Oudshoorn, C.; Mattace-roso, F. U.; van der Velde, N.; Colin, E. M.; van der Cammen, T. J. High serum vitamin D_3 levels are associated with better cognitive test performance in patients with Alzheimer's disease. *Dement Geriatr Dement Geriatr Cong Disord* 25: 539–543; 2008.

[16] Lúóng, K. V.; Nguyen, L. T. The beneficial role of vitamin D in Alzheimer's disease. *Am J Alzheimer's Dis Demen* 26: 511–520; 2011.

[17] Annweiler, C.; Beauchet, O. Vitamin D-mentia: randomized clinical trials should be the next step. *Neulopidemiology* 37: 249–258; 2011.

[18] Masoumi, A.; Goldenson, B.; Ghimai, S.; Avagyan, H.; Zaghi, J.; Abe, K.; Zheng, X.; Espinosa-Jeffrey, A.; Mahanian, M.; Liu, P. T.; Hewison, M.; Mizwickie, M.; Cashman, J.; Fiala, M. 1-alpha,25-Dihydroxyvitamin D_3 interacts with curcuminoids to stimulate amyloid-beta clearance by macrophages of Alzheimer's disease patients. *J Alzheimer's Dis* 17: 703–717; 2009.

[19] Veroniki, A. A.; Straus, S. E.; Ashoor, H. M.; Hamid, J. S.; Hemmelgarn, B. R.; Holroyd-Leduc, J.; Majumdar, S. R.; McAuley, G.; Tricco, A. C. Comparative safety and effectiveness of cognitive enhancers for Alzheimer's dementia: protocol for a systematic review and individual patient data network meta-analysis. *BMJ Open* 6: e010251; 2016.

[20] Goedert, M.; Spillantini, M. G. A century of Alzheimer's disease. *Science* 314: 777–781; 2006.

[21] Selkoe, D. J. Alzheimer's disease: a central role for amyloid. *J Neuropathol Exp Neurol.* 53: 438–447; 1994.

[22] Suzuki, N.; Cheung, T. T.; Cai, X. D.; Odaka, A.; Otvos, L. Jr; Eckman, C.; Golde, T. E.; Younkin, S. G. An increased percentage of long amyloid β protein secreted by familial amyloid β protein precursor (β APP717) mutants. *Science* 264: 1336–1340; 1994.

[23] Prior, R.; D'rso, D.; Frank, R.; Prikulis, I.; Cleven, S.; Ihl, R.; Pavlakovic, G. Selective binding of soluble Aβ1–40 and Aβ1–42 to a subset of senile plaques. *Am J Pathol* 48: 1749–1756; 1996.

[24] Glenner, G. G.; Wong, C. W. Alzheimer's disease: initial report of the purification and characterization of a novel cerebrovascular amyloid protein. *Biochem Biophys Res Commun* 120: 885–890; 1984.

[25] Goedart, M. Tau protein and the neurofibrillary pathology of Alzheimer's disease. *Trends Neurosci* 16: 460–465; 1993.

[26] Haass, C.; Selkoe, D. J. Soluble protein oligomers in neurodegeneration: lessons from the Alzheimer's amyloid beta-peptide. *Nat Mol Cell Biol* 8: 101–112; 2007.

[27] Kayed, R.; Head, E.; Thompson, J. L.; McIntire, T. M.; Milton, S. C.; Cotman, C. W.; Glabe, C. G. Common structure of soluble amyloid oligomers implies common mechanism of pathogenesis. *Science* 18: 486–489; 2003.

[28] Kuo, Y. M.; Emmerling, M. R.; Vigo-Pelfrey, C.; Kasunic, T. C.; Kirkpatrick, J. B.; Murdoch, G. H.; Ball, M. J.; Roher, A. E. Water-soluble Aβ;N-40, N-42 oligomers in normal and Alzheimer disease brains. *J Biol Chem* 271: 4077–4081; 1996.

[29] Collee, J. G.; Bradley, R.; Liberski, P. P. Variant CJD (vCJD) and bovine spongiform encepharopathy (BSE): 10 and 20 years on: part 2. *Foria Neuropathol* 44: 102–110; 2006.

[30] Prusiner, S. B. Prion diseases and crisis. *Science* 278: 245–251; 1997.

[31] Prusiner, S. B.; Bolton, D. C.; Groth, D. F.; Bowmann, K. A.; Choran, S. P.; Makinley, M. P. Further purification and characterization of scrapie prion. *Biochemistry* 21: 6942–6950; 1982.

[32] McKinley, M. P.; Masiarz, F. R.; Prusiner, S. B. Reversible chemical modification of the scrapie agent. *Science* 214: 1259–1261; 1998.

[33] Pan, K. M; Baldwin, M.; Nguyen, J.; Gasset, M.; Serban, A.; Groth, D.; Mehlhorn, I.; Hung, Z.; Fletterick, R. J.; Choen, F. E.; Prusiner, S. B. Conversion of alpha-helices into beta-sheets features in the formation of the scrapie prion proteins. *Proc Natl Acsd Sci USA* 90: 10962–10966; 1993.

[34] Rike, R.; Hornemann, S.; Wider, G.; Billeter, M.; Glockshuber, R.; Wuthrich, K. NMR structure of the mouse prion protein domain PrP(121–231). *Nature* 382: 180–182; 1996.

[35] James, T. L.; Liu, H.; Ulyanov, N. B.; Farr-Jones, S.; Zhang, H.; Donne, D. G.; Kaneko, K.; Groth, D.; Mehlhorn, I.; Prusiner, S. B.; Cohen, F. E. Solution structure of a 142-

residue recombinant prion protein corresponding to the infectious fragment of the scrapie isoform. *Proc Natl Acad Sci USA* 16: 10086–10091; 1997.

[36] Liu, H.; Farr-Jones, S.; Ulyanov, N. B.; Llinas, M.; Marqusee, S.; Groth, D.; Cohen, F. E.; Prusiner, S. B.; James, T. L. Solution structure of Syrian hamster prion protein rPrP(90–231). *Biochemistry* 38: 5362–5377; 1999.

[37] Prusiner, S. B. Molecular biology and pathogenesis of prion diseases. *Trends Biochem Sci* 252: 482–487; 1996.

[38] Collinge, J. Human prion disease and bovine spongiform encephalopathy (BSE). *Hum Mol Genet* 6: 1699–1705; 1997.

[39] Prusiner, S. B.; Scott, M.R.; DeArmond, S. J.; Cohen, F. E. Prion protein biology. *Cell* 93: 337–348; 1998.

[40] Choen, F. E.; Pan, K. M.; Hung, Z.; Baldwin, M.; Fletterick, R. J.; Prusiner, S. B. Structural clues to prion replication. *Science* 264: 530–531; 1994.

[41] Oesch, B.; Westaway, D.; Walchi, M.; et al. A cellular gene encodes scrapie PrP27–30 protein. *Cell* 40: 735–746; 1985.

[42] Bueler, H. R.; Aguzzi, A.; Sailer, A.; Greiner, R. A.; Austenried, O.; Aguet, M.; Weismann, C. Mice devoid of PrP are resistant to scrapie. *Cell* 73: 1339–1347; 1993.

[43] Rezaei, H. Prion protein oligomerization. *Curr Alzheimer Res* 5: 572–578; 2008.

[44] Kelly, J. W. The alternative conformations of amyloidogenic proteins and their multi-step assembly pathways. *Curr Opin Struct Biol* 8: 101–106; 1998.

[45] Chiti, F.; Dobson, C. M. Protein misfolding, functional amyloid, and human disease. *Annu Rev Biochem* 75: 333–366; 2006.

[46] Ebara, Y.; Itakura, K.; Okahata, Y. Kinetic studies of molecular recognition based on hydrogen bounding at the air-water interface by using a highly sensitive quartz-crystal microbalance. *Langmuir* 12: 5165–5170; 1996.

[47] Okuno, H.; Mori, K.; Jitsukawa, T.; Inoue, H.; Chiba, S. Convenient method for monitoring Aβ aggregation by quartz-crystal microbalance. *Chem Biol Drug Des* 68: 273–275; 2006.

[48] Sauerbrey, G. Verwendrug von Schwingquarzen zur Wagung dunner Schichten, und zur Mikrowagun. *Z Phys* 155: 206–222; 1959.

[49] Suenaga, M.; Takahashi, H.; Imagawa, H.; Wagatsuma, M.; Ouma, S.; Tsuboi, Y.; Furuta, A.; Matsunaga, Y. Different effect of vitamin D_2 and vitamin D_3 on amyloid-β40 aggregation in vitro. *Curr Altz Res* 11: 745–754; 2014.

[50] Biancalana, M.; Koide, S. Molecular mechanism of thioflavin-T binding to amyloid fibrils. *Biochem Biophys Acta* 1804: 1405–1412; 2010.

[51] Levine, H. 3rd. Quantification of β-sheet amyloid fibril structures with thioflavin T. *Methods Enzymol* 309: 274–284; 1999.

[52] Suenaga, M.; Hiramoto, Y.; Matsunaga, Y. Vitamin D_2 interacts with human PrP^c(90–231) and breaks PrP^c oligomerization in vitro. *PRION* 7: 1–7; 2013.

[53] Tjernberg, L. O.; Naslund, J.; Lindqvist, F.; Johansson, J.; Karlstrom, A. R.; Thyberg, J.; Terenius, L.; Nordstedt, C. Controlling amyloid β peptide fibril formation with protease-stable ligands. *J Biol Chem* 272: 12601–12605; 1997.

[54] Matsunaga, Y.; Saito, N, Fujii, A.; Yokutani, J.; Takakura, T.; Nishimura, T.; Esaki, H.; Yamada, T. A pH-dependent conformational transition of Aβ peptide and physico-chemical properties of the conformers in the glial cell. *Biochem J* 361: 547–556; 2002.

[55] Hatip, F. F.; Suenaga, M.; Yamada, T.; Matsunaga, Y. Reversal of temperature-induced conformational changes in the amyloid-beta peptide, Aβ40, by the β-sheet breaker peptides 16–23 and 17–24. *J Pharmacol* 158: 1165–1172 ; 2009.

[56] Matsunaga, Y.; Peretz, D.; Williamson, A.; Burton, D.; Mehlhorn, I.; Groth, D.; Cohen, F. E.; Prusiner, S. B.; Baldwin, M. Cryptic epitopes in N-terminally truncated prion protein are exposed in the full-length molecule: dependence of conformation on pH. *Protein* 44: 110–118; 2001.

[57] Hoffmann, R. W. Allylic 1,3-strain as a controlling factor in stereoselective transformations. *Chem Rev* 89: 1841–1860; 1989.

[58] Wiberg, K. B.; Martin, E. Barriers to rotation adjacent to double bonds. *J Am Chem Soc* 107: 5035–5041; 1985.